

High-average-power, high-repetition-rate tunable terahertz difference frequency generation with GaSe crystal pumped by 2 μm dual-wavelength intracavity KTP optical parametric oscillator

DEXIAN YAN,^{1,2} YUYE WANG,^{1,2,3,5} DEGANG XU,^{1,2,6} PENGXIANG LIU,^{1,2} CHAO YAN,^{1,2} JIA SHI,^{1,2} HONGXIANG LIU,^{1,2} YIXIN HE,^{1,2} LONGHUANG TANG,^{1,2} JIANCHEN FENG,^{1,2} JIANQIN GUO,^{1,2} WEI SHI,^{1,2} KAI ZHONG,^{1,2} YUEN H. TSANG,⁴ AND JIANQUAN YAO^{1,2}

¹School of Precision Instrument and Opto-electronics Engineering, Tianjin University, Tianjin 300072, China

²Key Laboratory of Opto-electronics Information Technology, Tianjin University, Ministry of Education, Tianjin 300072, China

³Institute of Neurosurgery, Southwest Hospital, Third Military Medical University, Chongqing 400038, China

⁴Department of Applied Physics, the Hong Kong Polytechnic University, Hong Kong, China

⁵e-mail: yuyewang@tju.edu.cn

⁶e-mail: xudegang@tju.edu.cn

Received 5 December 2016; revised 25 January 2017; accepted 27 January 2017; posted 31 January 2017 (Doc. ID 282184); published 20 February 2017

We have demonstrated a high-average-power, high-repetition-rate optical terahertz (THz) source based on difference frequency generation (DFG) in the GaSe crystal by using a near-degenerate 2 μm intracavity KTP optical parametric oscillator as the pump source. The power of the 2 μm dual-wavelength laser was up to 12.33 W with continuous tuning ranges of 1988.0–2196.2 nm/2278.4–2065.6 nm for two waves. Different GaSe crystal lengths have been experimentally investigated for the DFG THz source in order to optimize the THz output power, which was in good agreement with the theoretical analysis. Based on an 8 mm long GaSe crystal, the THz wave was continuously tuned from 0.21 to 3 THz. The maximum THz average power of 1.66 μW was obtained at repetition rate of 10 kHz under 1.48 THz. The single pulse energy amounted to 166 pJ and the conversion efficiency from 2 μm laser to THz output was 1.68×10^{-6} . The signal-to-noise ratio of the detected THz voltage was 23 dB. The acceptance angle of DFG in the GaSe crystal was measured to be 0.16° . © 2017 Chinese Laser Press

OCIS codes: (140.3070) Infrared and far-infrared lasers; (190.4223) Nonlinear wave mixing; (190.4410) Nonlinear optics, parametric processes; (260.3090) Infrared, far.

<https://doi.org/10.1364/PRJ.5.000082>

1. INTRODUCTION

The advent of laser-based coherent terahertz (THz) radiation has attracted much attention for its potential applications in spectrum analysis, biological detection, and imaging systems [1–3]. From the perspective of practical applications of THz technologies, high-average power, high-repetition-rate THz waves are still in great demand for near-field microscopy, high-resolution spectroscopy, and hyper-spectral imaging systems. Optical rectification (OR) is an effective method to generate high-repetition-rate THz waves [4,5]. It has utilized the ultra-broad-bandwidth characteristics of femtosecond optical pulses, so that the generated THz waves possess high temporal characteristics with the sacrifice of their narrowband spectrum in the frequency domain. Different from OR, difference frequency generation (DFG) between two close laser

wavelengths in nonlinear crystals is a proven approach for coherent THz wave generation, which can offer relative compactness, flexible tunability, and stable and narrowband THz output [6–12]. The pump light is usually continuous wave (CW) and nanosecond pulses. Moreover, another obvious advantage of a nonlinear DFG scheme is that the generated THz power is scalable with high-power pump lasers and proper nonlinear crystals with sufficient physical parameters. Until now, considerable effort has been made to improve the performance of optical THz sources from different aspects: nonlinear crystals, phase-matching (PM) configurations, and dual-wavelength pump sources.

The GaSe crystal is one of the widely used superior nonlinear crystals for efficient THz generation, due to the characteristics of high second-order nonlinear optical coefficient

($d_{22} = 54 \text{ pm/V}$), lower absorption coefficients in the THz wavelength region, and better transparency from 0.6 to 20 μm . Considering that the effective nonlinear coefficient for Type-II (oe) DFG in GaSe is $d_{\text{eff}} = d_{22} \cos 2\theta \cos(3\varphi)$, $\varphi = 0^\circ$ was applied for the maximum conversion efficiency, and PM can be realized by simply rotating the crystal in the x - z plane. To date, most pump sources of monochromatic DFG THz systems utilize two separate laser cavities or gain media to generate two different wavelengths. The systems are thus complex in mechanical alignment, and the spatial overlap of laser transverse modes is poor [11,13]. Considering that GaSe crystal has a bandgap of about 2.2 eV, it will be beneficial for avoiding the two-photon absorption using the pumping laser at 2 μm . In particular, on the basis of the Manley-Rowe relation, employing 2 μm dual-wavelength pump lasers for DFG can double the quantum efficiency compared with that using 1 μm pump lasers. Over the past few years, dual-wavelength operation around 2 μm lasers has been achieved with several approaches, including Tm-doped, Ho³⁺-doped, and Tm³⁺:Ho³⁺ co-doped fiber lasers; mode-locked Tm:CaYAlO₄ (Tm:CYA) lasers; and a solid-state 1 μm Nd laser with a degenerate optical parametric oscillator (OPO). Because the high-power tunable mid-IR output with solid-state or fiber lasers is difficult, 2 μm dual-wavelength lasers generated with nearly degenerate OPO pumped by 1.06 μm Nd:YAG lasers is the promising alternative approach. Since 2010, our group has focused on DFG THz sources pumped by pulsed 2 μm dual-wavelength lasers [14–16]. However, the relatively low repetition rate of typically 10 Hz restricts the sensitivity of experiments to those phenomena that exhibit rather drastic changes in the transient linear optical properties of the samples. In 2016, Mei *et al.* first reported high-repetition-rate THz generation based on DFG in GaSe crystal using the diode-end-pumped dual-wavelength KTP OPO around 2 μm [17,18]. The single pulse energy of the THz wave was about 48 pJ at 1.54 THz and the DFG conversion efficiency was 7.8×10^{-7} . In view of the thermal stress inducing fractures of the laser crystal, the THz output power scaling is limited with the end-pumped laser system. In comparison, the side-pumped configuration is useful for the purpose of power scaling because, in this configuration, a longer laser crystal rod can be used and pump power can be easily scaled with multiple diode arrays around the outside of the laser rod or along its axis.

The aim of this work is to achieve high-average-power, high-repetition-rate, and tunable THz sources based on DFG with GaSe crystals. A high-peak-power dual-wavelength 2 μm laser was experimentally obtained with intracavity KTP OPO pumped by diode-side-pumped acousto-optic (AO) Q-switched Nd:YAG laser. Two identical KTP crystals were oriented oppositely in the OPO cavity to compensate for the walk-off effect. Maximum average power of 12 W for a 2 μm laser has been obtained with peak power of more than 100 kW. Two GaSe crystals with the lengths of 8 and 15 mm were experimentally investigated for DFG in order to optimize the THz output power. The results were in good agreement with the theoretical analysis. By using the 8 mm long GaSe crystal, a THz tunable range from 0.21 to 3 THz was achieved.

The maximum THz average power reached 1.66 μW with repetition rate of 10 kHz at 1.48 THz under 2 μm dual-wavelength pump power of 2.1 W, corresponding to single pulse energy of 166 pJ and conversion efficiency of 1.68×10^{-6} . Meanwhile, the signal-to-noise ratio (SNR) of THz voltage was up to 23 dB as detected by a 4.2 K Si bolometer. The acceptance angle of DFG with the 8 mm long GaSe crystal was measured to be 0.16° . This study has provided new performance for a GaSe DFG THz source based on an intracavity diode-side-pumped 2 μm dual-wavelength laser. Such a high-average-power THz wave source at elevated repetition rates can be applied to fast data sampling in frequency-resolved experiments for many applications, such as near-field microscopy, high-resolution spectroscopy, or hyper-spectral imaging systems.

2. EXPERIMENTAL SETUP

The experimental setup is illustrated in Fig. 1. The intracavity KTP OPO was pumped by a diode-side-pumped AO Q-switched Nd:YAG laser. The pump module consists of five diode stacked arrays emitting at 808 nm, which were arranged in a pentagonal shape around the rod to reach better pumping uniformity. A Nd:YAG rod with 3 mm in diameter and 65 mm in length was plane-parallel polished and antireflection (AR) coated on both ends at 1.06 μm . The rear mirror (M1) was a 2000 mm radius-of-curvature concave mirror with reflectivity of 99.5% at 1.06 μm . An AO modulator (Gooch and Housego Inc., UK) with high diffraction efficiency was used as the Q-switch and placed between M1 and the Nd:YAG rod. Its repetition rate was optimized to be 10 kHz with respect to the OPO average output power. The plane parallel output mirror (M3) had highly reflective (HR) coatings ($R > 99.8\%$) at 1.06 μm and partial transmission ($T = 25\%$) coatings in the range of 2–2.3 μm . A plane-concave cavity structure was employed to compensate for the thermal effect and improve stability and efficiency. The overall 1.06 μm laser cavity was 350 mm long and was formed by two mirrors, M1 and M3. The intracavity OPO cavity, 55 mm in length, was formed by two flat mirrors, M2 and M3, and two identical KTP crystals (CSK Photonics Co. Ltd., Jinan, China). Flat quartz mirror M2 was HR coated at 2–2.3 μm and AR coated at 1.06 μm . The KTP crystals, with dimensions of 7 mm \times 8 mm \times 15 mm, were AR coated at 1.06 μm and resonant wavelengths of 2–2.3 μm . They were placed between mirror M2 and output mirror M3. The two KTP crystals, with

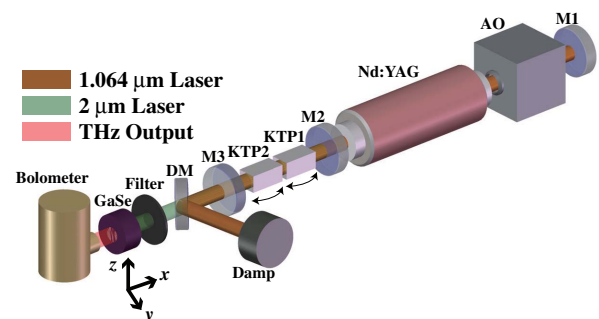


Fig. 1. Experimental setup of the THz DFG with GaSe crystals.

PM angles of $\theta = 51.2^\circ$, $\varphi = 0^\circ$, were oriented oppositely in the OPO cavity to compensate for the walk-off effect, and they were symmetrically tuned in the x - z plane to achieve type-II ($o \rightarrow e + o$) PM. They were wrapped with indium foil and mounted in two water-cooled copper blocks whose surface temperature was kept at about 17°C .

After filtering out the residual $1.06\ \mu\text{m}$ laser by a dichromatic mirror (DM) (HR at $1.06\ \mu\text{m}$ and AR at 1.8 – $2.5\ \mu\text{m}$), the $2\ \mu\text{m}$ dual-wavelength laser beam was chopped using an optical chopper (Stanford Research Systems, SR540) with a 50% duty cycle at a frequency of 50 Hz, and then it was injected into the GaSe crystal. We used two commercial GaSe crystals with lengths of 8 and 15 mm; they were uncoated at both faces for DFG and were 16 mm in diameter. The THz frequency was calculated from the difference between the two measured frequencies of the $2\ \mu\text{m}$ dual-wavelength laser. The generated THz wave was detected by 4.2 K helium cooled Si bolometer (IR-labs Inc.). A 1 mm germanium (Ge) wafer and a 1 mm black polyethylene (PE) wafer were used together to filter out the near-IR radiation and the undesired background light.

3. RESULTS AND DISCUSSION

Figure 2(a) shows average output power of the 1.06 and $2\ \mu\text{m}$ dual-wavelength lasers versus electric input power, and optical-to-optical conversion efficiency from the 1.06 to the $2\ \mu\text{m}$ laser. Before adding the intracavity OPO, the electric pump thresholds of the $1.06\ \mu\text{m}$ laser operating at CW and Q-switched modes were 180 and 182 W, respectively. Then, the electric pump threshold of the $2\ \mu\text{m}$ dual-wavelength OPO was 197 W. The pump threshold difference between the operations of the 1.06 and $2\ \mu\text{m}$ dual-wavelength lasers can be explained by cavity loss introduced by the OPO cavity. The conversion efficiency of the 1.06 to $2\ \mu\text{m}$ dual wavelengths was about 20%. Figure 2(b) shows the tuning characteristics of the dual-wavelength $2\ \mu\text{m}$ laser under electrical input power of 470 W. The output of the KTP OPO contained two orthogonal linear polarization states. By symmetrically tuning the PM angle of the two KTPs in the x - z plane, the ordinary light (o-light) of the $2\ \mu\text{m}$ dual-wavelength laser can be continuously tuned to cover the range from 1988.0 to 2196.2 nm, and the extraordinary light (e-light) can be continuously tuned to cover

the range from 2278.4 to 2065.6 nm simultaneously. This can generate tunable THz output from 0.01 to 20 THz. From Fig. 2(b), it can be found that the degeneracy occurred at PM angle of 51.08° with output wavelength of 2128.6 nm, whereas the theoretical calculated value is 50.8° [19]. The small difference could be attributed to the general Sellmeier equation used for the KTP crystals, inexactitude in KTP crystal cutting, and measurement errors for the PM angle. The maximum output power of 12.33 W for the $2\ \mu\text{m}$ dual-wavelength laser occurred at 51.2° . There was slight variance for the output power as PM angle tuning. This phenomenon was likely to be caused by the increased Fresnel reflection loss at KTP faces and thermal-induced cavity instability while tuning the PM angle.

The OPO output spectrum measured by the optical spectrum analyzer (Yokogawa AQ6375) are shown in Fig. 3(a), which shows dual wavelengths of 2118.1 and 2140.5 nm simultaneously. The insets indicate that the full widths at half-maximum (FWHM) for two wavelengths are as narrow as 0.8 nm. A Glan-Taylor prism was used to separate the output beam into o-light and e-light. The temporal pulse shapes of the KTP OPO detected by the fast response InGaAs PIN detector (EOT ET-5000) are given in Fig. 3(b), where the inset shows the pulse shape of the $1.06\ \mu\text{m}$ laser. It is seen that the pulse widths of the two independent separated wavelengths and the combined dual wavelength were all around 11 ns under electric input power of 470 W, much narrower than that of the $1.06\ \mu\text{m}$ laser (70 ns). Moreover, the timing jitter of the dual-wavelength laser was negligible. Benefiting from the walk-off compensating arrangement of the two KTP crystals, beam quality factor (M^2) values of the $2\ \mu\text{m}$ dual-wavelength laser were 3.0 and 3.4 for the vertical and horizontal directions, respectively. The beam size for the horizontal direction and vertical direction were 2.3 and 1.8 mm, respectively. The divergence angles were 0.126° and 0.1° for the vertical and horizontal directions, respectively.

A GaSe crystal with length of 8 mm was placed directly after the DM filter. The optimal PM conditions can be realized for DFG by rotating in the x - z plane and optimizing the position of the GaSe crystal. Figure 4 shows the relationship between the generated THz wavelength with respect to the external PM angles for the type-II (o - $e \rightarrow e$) collinear DFG. Circles and the solid curve represent the experimental result and theoretical simulation using Sellmeier equations [20]. The experimental

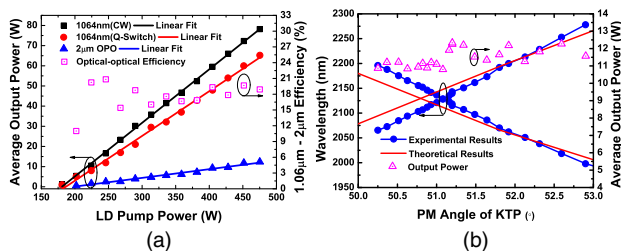


Fig. 2. (a) Output power of the Nd:YAG laser and $2\ \mu\text{m}$ KTP OPO versus electric input power as well as 1.06 to $2\ \mu\text{m}$ dual-wavelength conversion efficiency. (b) Angle tuning characteristics of the KTP OPO. The blue circles and the red solid line represent the experimental and theoretical results, respectively. Triangles indicate the $2\ \mu\text{m}$ dual-wavelength laser power with respect to related PM angles of KTP.

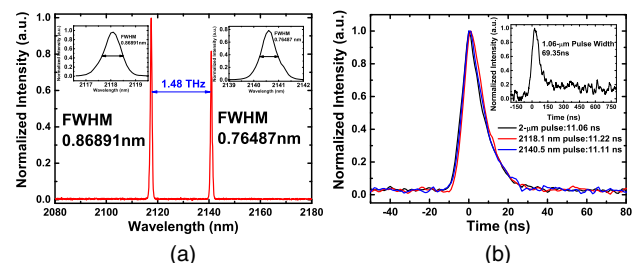


Fig. 3. (a) Dual-wavelength spectra of the $2\ \mu\text{m}$ pump source of the DFG (the insets show the FWHM of the two wavelengths). (b) Temporal pulse profile for the combined dual wavelengths and the two independent separated wavelengths of 2118.1 and 2140.5 nm. The inset shows the pulse shape of the $1.06\ \mu\text{m}$ laser.

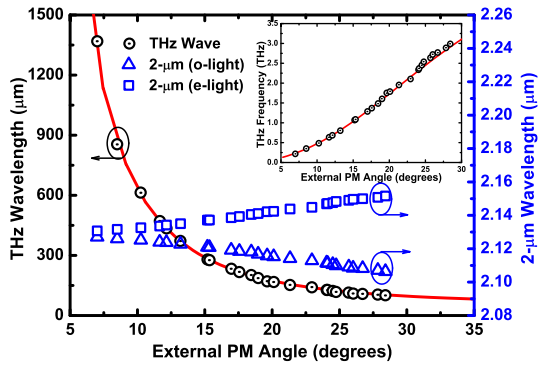


Fig. 4. THz wavelengths versus external PM angles. Inset: THz frequency versus external PM angles. Circles and the solid curve represent the experimental and theoretical results, respectively. Squares and triangles represent the 2 μm wavelength used for DFG THz.

data of the 2 μm dual-wavelength laser for determining the THz wavelength is shown in Fig. 4. A coherent THz wave with tuning range from 100 to 1428.57 μm was achieved when the two pump waves were tuned in the range of 2106.4 to 2127.2 nm for o-light and 2151.6 to 2130.4 nm for e-light. The corresponding THz output frequency from 0.21 to 3 THz is shown in the inset. The high-frequency end was limited by the rapidly increased absorption coefficient of the GaSe crystal and the decreased conversion efficiency with the increase of PM angle.

The THz output power was measured using 4.2 K helium-cooled Si bolometer, which was calibrated to 2.89×10^5 V/W and connected to a digital oscilloscope to read the signal intensity. Two crystals with lengths of 8 and 15 mm have been used in our experiments. Figure 5(a) shows the THz output voltage versus THz frequency tuning range under 2 μm dual-wavelength pump power of about 950 mW, where two curves have similar variation tendency. For the 8 mm long GaSe crystal, the tuning range from 0.21 to 3 THz was obtained. The measured maximum output voltage was 2.24 V at frequency of 1.48 THz (202.40 μm in wavelength). The corresponding THz average power was 0.78 μW at a repetition rate of 10 kHz. For the 15 mm long GaSe crystal, the tuning range

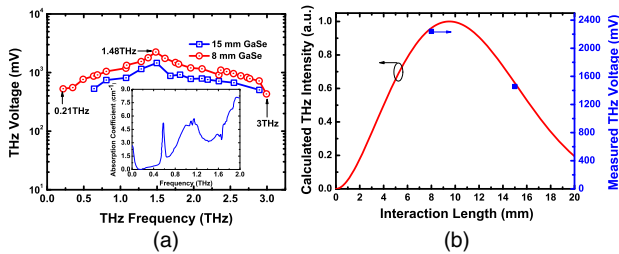


Fig. 5. (a) THz output voltage versus THz frequency for two GaSe crystals with different lengths under 2 μm dual-wavelength pump power of about 950 mW. (b) Calculated THz intensity (solid curve) and measured THz voltages (squares) of the DFG THz source versus the interaction length at 1.48 THz. The inset shows the absorption coefficient of our GaSe crystal measured with a THz time domain system.

was from 0.64 to 2.89 THz. The maximum output voltage was 1.46 V at 1.48 THz, and the corresponding THz average power was 0.51 μW under 10 kHz. Therefore, it can be concluded that higher THz output power and wider tuning range could be obtained with a shorter GaSe crystal. The power of the THz wave generated from GaSe crystal is affected by the absorption coefficient. The inset of Fig. 5(a) shows the absorption coefficient of our 8 mm long GaSe crystal measured with a THz time domain system (Advantest Co., TAS7500). The maximum power is obtained at the window with relatively low absorption in the GaSe crystal. We analyzed the dependence of the output at 1.48 THz with respect to the interaction length in GaSe crystal, based on the coupled equations of three-wave interaction [21]. The detailed calculation process is described in Refs. [16,21]. In the calculation, the pump power of 950 mW, GaSe crystal absorption coefficient of 3.3 cm^{-1} , and other parameters obtained in our work were used. The calculated THz intensity (solid curve) and measured THz voltages (squares) of the DFG THz source versus the interaction length at 1.48 THz are shown in Fig. 5(b). It can be deduced that there exists an optimum length of the GaSe crystal for obtaining the maximum THz output. The normalized THz intensity for the 8 mm long GaSe crystal is 1.52 times that with the 15 mm long GaSe crystal. This is in good agreement with our experimental results, indicated by squares in Fig. 5(b). In addition, the THz intensity first increases, and then drops with the interaction length increasing. This is because of the increased absorption of the THz wave and the pump depletion with the longer crystal. In addition, when the longer GaSe crystal is rotated, it could lead to more obvious separation of the dual wavelengths under non-normal incidence, which will deteriorate the collinear PM configuration and reduce the THz conversion efficiency.

When the THz frequency was 1.48 THz, the input–output characteristic with the 8 mm long crystal is shown in Fig. 6. The THz output voltage and average power exhibited a quadratic relationship (solid line) with respect to the 2 μm dual-wavelength pump power, which satisfies the characteristic for DFG. Under incident 2 μm dual-wavelength pump power of 2.1 W, a THz output voltage of 4.8 V was achieved,

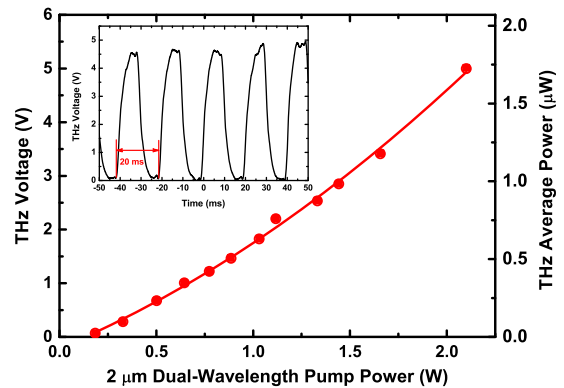


Fig. 6. Dependences of THz voltages and average power on the 2 μm dual-wavelength pump power. The red line is a quadratic fit of experimental data points. The inset shows the THz signal detected by using the 4.2 K Si bolometer.

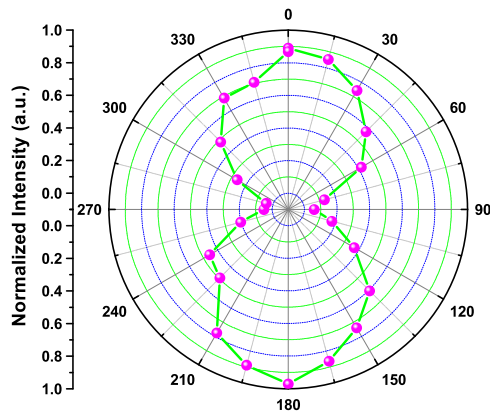


Fig. 7. THz intensity as a function of the rotation angle of the THz polarizer at 1.48 THz.

corresponding to the THz average power of $1.66 \mu\text{W}$. The highest conversion efficiency from the $2 \mu\text{m}$ input laser to THz output power reached 1.68×10^{-6} , and the corresponding photon conversion efficiency was 1.6×10^{-4} . When the incident $2 \mu\text{m}$ dual-wavelength pump power was further improved, unfortunately, the GaSe crystal was damaged. Therefore, improvement of the damage threshold of the GaSe crystal and reduction of the thermal effect in the system are necessary. The THz signal detected by the 4.2 K Si bolometer is shown in the inset, from which we can see that the duration of one signal envelope was 20 ms, owing to the chopping frequency of 50 Hz and high-repetition-rate THz operation. Moreover, the modulated THz signal pulse at 1.48 THz was relatively stable and the pulse-to-pulse amplitude fluctuation was estimated to be less than 5%. The SNR of the THz voltage detected by the bolometer was detected to be 23 dB. According to the measured pulse width and linewidth of the $2 \mu\text{m}$ dual-wavelength pump laser above, the pulse width and linewidth of the THz wave was estimated to be about 10 ns and 50.0 GHz, respectively [10].

To confirm the polarization direction of the generated THz wave, a wire grid polarizer (MicroTech Instruments, Inc.) was used. The maximum transmission should appear when the THz polarization is perpendicular to the orientation of the wire grid (90° or 270°). Figure 7 shows the THz intensity at 1.48 THz under different rotation angles of the polarizer. It is seen that the THz wave is linearly polarized. Also, the polarization of the THz wave was the same as that of the longer pump wavelength (e-light), which is in good agreement with the type-II (o-e \rightarrow e) PM in DFG.

Finally, the acceptance external PM angle of the GaSe crystal at 1.48 THz was analyzed, as shown in Fig. 8. For type-ooe PM in GaSe crystal, the acceptance PM angle $\Delta\theta$ is

$$\Delta\theta = \frac{1}{l} \frac{1}{[(n_{2e} - n_{2o})/\lambda_{p2} + (n_{\text{THze}} - n_{\text{THzo}})/\lambda_{\text{THz}}] \sin 2\theta_p}, \quad (1)$$

where l is the length of the GaSe crystal. It should be mentioned that the linewidth of the $2 \mu\text{m}$ pump light, the divergence angle of the pump light, and the refractive index changes of the DFG

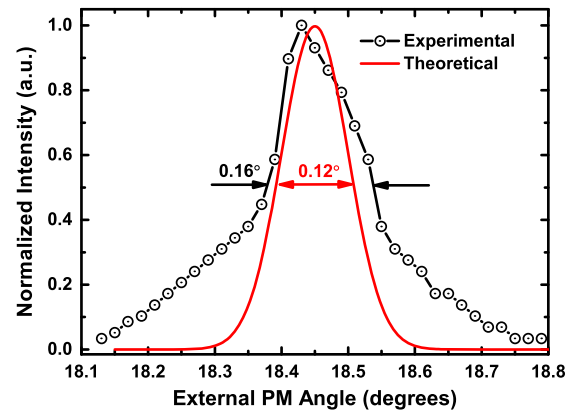


Fig. 8. Accepted PM angle of the GaSe crystal at 1.48 THz.

crystal induced by temperature change are ignored in Eq. (1). The theoretical value for the external acceptance PM angle is 0.12° at crystal temperature of 25°C , whereas the measured value is 0.16° . The difference can be attributed to the variable DFG crystal temperature under high-repetition-rate operation, the divergence angle of about 0.1° , and a certain linewidth of the $2 \mu\text{m}$ pump laser ($\sim 0.8 \text{ nm}$).

4. CONCLUSION

A high-average-power, high-repetition-rate optical THz source based on DFG in GaSe crystal has been demonstrated by using a near-degenerate $2 \mu\text{m}$ KTP OPO as the pump source. The dual wavelength of the intracavity OPO was in the range of 1988.0 to 2196.2 nm for o-light and 2278.4 to 2065.6 nm for e-light while symmetrically tuning the PM angle of two KTPs. Two GaSe crystals with lengths of 8 and 15 mm were experimentally investigated for DFG in order to optimize the THz output power. The result was in good agreement with the theoretical analysis. By using the 8 mm long GaSe crystal, a THz tunable range from 0.21 to 3 THz was achieved. The highest average power and optical-to-THz conversion efficiency at 1.48 THz were $1.66 \mu\text{W}$ and 1.68×10^{-6} , respectively. The single pulse energy reached 166 pJ under the repetition rate of 10 kHz. Meanwhile, the SNR of the THz voltage was up to 23 dB as detected by a 4.2 K Si bolometer. The acceptance angle was measured to be 0.16° . It is expected that such a high-power, high-repetition-rate tunable THz source can provide good advantages and find numerous applications in the thorough research of THz waves in the future.

Funding. National Basic Research Program of China (973) (2014CB339802, 2015CB755403); National key research and development projects (2016YFC0101001); National Key Technology R&D Program of China (2014BAI04B05, 2015BAI01B01); National Natural Science Foundation of China (NSFC) (61107086, 61471257, 81402067); Natural Science Foundation of Tianjin City (14JCQNJC02200); Postdoctoral Science Foundation of Chongqing (Xm2016021); Joint Incubation Project of Southwest Hospital (SWH2016LHJC-04, SWH2016LHJC-01); Science and Technology Support Program of Tianjin (13ZCZDSF02300).

REFERENCES

1. A. Lee, Y. He, and H. Pask, "Frequency-tunable THz source based on stimulated polariton scattering in Mg:LiNbO₃," *IEEE J. Quantum Electron.* **49**, 357–364 (2013).
2. M. Tonouchi, "Cutting-edge terahertz technology," *Nat. Photonics* **1**, 97–105 (2007).
3. G. Davies, A. D. Burnett, W. Fan, E. H. Linfield, and J. E. Cunningham, "Terahertz spectroscopy of explosives and drugs," *Mater. Today* **11**, 18–26 (2008).
4. W. C. Chu, S. A. Ku, H. J. Wang, C. W. Luo, Y. M. Andreev, G. Lanski, and T. Kobayashi, "Widely linear and non-phase-matched optical-to-terahertz conversion on GaSe:Te crystals," *Opt. Lett.* **37**, 945–947 (2012).
5. S. A. Ku, W. C. Chu, C. W. Luo, Y. M. Andreev, G. Lanski, A. Shaidukoi, T. Izaak, V. Svetlichnyi, K. H. Wu, and T. Kobayashi, "Optimal Te-doping in GaSe for non-linear applications," *Opt. Express* **20**, 5029–5037 (2012).
6. W. Shi, Y. J. Ding, N. Fernelius, and K. L. Vodopyanov, "An efficient, tunable, and coherent 0.18–5.27 THz source based on GaSe crystal," *Opt. Lett.* **27**, 1454–1456 (2002).
7. M. Tang, H. Minamide, Y. Y. Wang, T. Notake, S. Ohno, and H. Ito, "Tunable terahertz-wave generation from DAST crystal pumped by a monolithic dual-wavelength fiber laser," *Opt. Express* **19**, 779–786 (2011).
8. M. Tang, H. Minamide, Y. Y. Wang, T. Notake, S. Ohno, and H. Ito, "Dual-wavelength single-crystal double-pass KTP optical parametric oscillator and its application in terahertz wave generation," *Opt. Lett.* **35**, 1698–1700 (2010).
9. T. Tanabe, K. Suto, J. Nishizawa, K. Saito, and T. Kimura, "Frequency-tunable terahertz wave generation via excitation of phonon-polaritons in GaP," *J. Phys. D* **37**, 155–158 (2003).
10. P. Zhao, S. Ragam, Y. J. Ding, and I. B. Zotova, "Compact and portable terahertz source by mixing two frequencies generated simultaneously by a single solid-state laser," *Opt. Lett.* **35**, 3979–3981 (2010).
11. P. Zhao, S. Ragam, Y. J. Ding, and I. B. Zotova, "Power scalability and frequency agility of compact terahertz source based on frequency mixing from solid-state lasers," *Appl. Phys. Lett.* **98**, 131106 (2011).
12. T. Tanikuchi, J. I. Shikata, and H. Ito, "Continuously tunable THz-wave generation from GaP crystal by difference frequency mixing with a dual-wavelength KTP-OPO," in *8th International Conference on Terahertz Electronics* (2000), pp. 225–228.
13. K. Nawata, T. Abe, Y. Miyake, A. Sato, K. Asai, H. Ito, and H. Minamide, "Efficient terahertz-wave generation using a 4-dimethylamino-N-methyl-4-stilbazolium tosylate pumped by a dual-wavelength neodymium-doped yttrium aluminum garnet laser," *Appl. Phys. Express* **5**, 112401 (2012).
14. K. Zhong, J. Q. Yao, D. G. Xu, Z. Wang, Z. Y. Li, H. Y. Zhang, and P. Wang, "Enhancement of terahertz wave difference frequency generation based on a compact walk-off compensated KTP OPO," *Opt. Commun.* **283**, 3520–3524 (2010).
15. D. G. Xu, W. Shi, K. Zhong, Y. Y. Wang, P. X. Liu, and J. Q. Yao, "The widely tunable THz generation in QPM-GaAs crystal pumped by a near-degenerate dual-wavelength KTP OPO at around 2.127 μm ," *Proc. SPIE* **8604**, 86040 (2013).
16. P. X. Liu, X. Y. Zhang, C. Yan, D. G. Xu, Y. Li, W. Shi, G. C. Zhang, X. Z. Zhang, J. Q. Yao, and Y. C. Wu, "Widely tunable and monochromatic terahertz difference frequency generation with organic crystal 2-(3-(4-hydroxystyryl)-5, 5-dimethylcyclohex-2-enylidene) malononitrile," *Appl. Phys. Lett.* **380**, 621–627 (2016).
17. J. L. Mei, K. Zhong, M. R. Wang, Y. Liu, D. G. Xu, W. Shi, Y. Y. Wang, J. Q. Yao, A. N. Robert, and P. Nasser, "Widely-tunable high-repetition-rate terahertz generation in GaSe with a compact dual-wavelength KTP OPO around 2 μm ," *Opt. Express* **24**, 23368–23375 (2016).
18. J. L. Mei, K. Zhong, M. R. Wang, P. X. Liu, D. G. Xu, Y. Y. Wang, W. Shi, J. Q. Yao, A. N. Robert, and P. Nasser, "High-repetition-rate terahertz generation in QPM GaAs with a compact efficient 2- μm KTP OPO," *IEEE Photon. Technol. Lett.* **28**, 1501–1504 (2016).
19. K. Kato, "Parametric oscillation at 3.2 μm in KTP pumped at 1.064 μm ," *IEEE J. Quantum Electron.* **27**, 1137–1140 (1991).
20. K. L. Vodopyanov and L. A. Kulevskii, "New dispersion relationships for GaSe in the 0.65–18 μm spectral region," *Opt. Commun.* **118**, 375–378 (1995).
21. P. E. Powers, *Fundamentals of Nonlinear Optics* (CRC Press, 2011).